Optimizing magnetomotive contrast of SPIO-labeled platelets for thrombosis imaging in optical coherence tomography

Amy L. Oldenburg[a,b], Dmitry Spivak[a], Gongting Wu[a], Frank Tsui[a], Thomas H. Fischer[c]
[a]University of North Carolina at Chapel Hill, Department of Physics and Astronomy, CB 3255, Chapel Hill, NC, USA 27599-3255;
[b]University of North Carolina at Chapel Hill, Biomedical Research Imaging Center, Chapel Hill, NC, USA 27599;
[c]University of North Carolina at Chapel Hill, Department of Pathology and Laboratory Medicine, Chapel Hill, NC, USA 27599-7525

ABSTRACT

Rehydratable, lyophilized platelets loaded with superparamagnetic iron oxides (SPIOs) has the potential to provide magnetomotive imaging contrast to sites of vascular damage, including thrombosis complicating atherosclerosis and hemorrhage. Magnetomotive optical coherence tomography (MMOCT) contrasts SPIO-platelets based on their nanoscale, magnetically-induced motion. We report improvements in MMOCT imaging contrast and sensitivity by optimizing the magnetic properties and SPIO loading of the platelets. SPIO-platelets have been shown to specifically adhere to sites of vascular damage in porcine arteries *ex vivo*. This may lead to new methods for detecting internal bleeding and monitoring the formation of blood clots using infused SPIO-platelets.

Keywords: Magnetomotive Optical Coherence Tomography, Platelets, Superparamagnetic iron oxide

1. INTRODUCTION

Clotting at sites of vascular damage is the source of cardiovascular events and the driver of thrombotic complications. Optical coherence tomography (OCT) is increasingly employed as an intravascular imaging modality to provide high-resolution imaging of vascular lesions, such as in the coronary artery for identifying unstable plaques [1, 2], vascular conduit quality during bypass surgery [3], and assessing balloon inflation during angioplasty [4]. However, OCT image contrast is based upon coherent backscattering, which is not highly modulated by vascular pathology or function. New OCT-based methods for contrasting thrombosis would leverage these current technologies for *in vivo* imaging while providing the needed tools for functional imaging.

We have recently reported a new method for thrombosis imaging based on the use of infusible, rehydratable, lyophilized (RL) platelets carrying a payload of superparamagnetic iron oxides (SPIOs) which are contrasted using magnetomotive optical coherence tomography (MMOCT) [5]. RL platelets are infusion agent that are prepared from fresh human apheresis platelets and overcome difficulties with platelet storage and harvesting [6, 7]. They have been shown to reduce bleeding times in animal models [8]. Because blood itself is not highly magnetic when volume-averaged [9], RL platelets can be loaded with SPIOs in sufficient quantity to provide contrast in MMOCT. MMOCT is a method for tracking magnetic particle-loaded cells [10, 11]. Current phase-sensitive implementations of MMOCT are based on tracking the modulated motion of SPIOs in the phase of the spectral-domain OCT signal, resulting in nanomolar sensitivity [12]. Some recent applications of MMOCT have been for hemoglobin contrast [13], macrophage identification [14, 15], targeted breast cancer imaging [16], and optical rheology [17].

Importantly, we find that SPIO-RL platelets maintain their ability to specifically localize to injured vasculature, and do so in sufficient quantity for detection by MMOCT, as demonstrated in an *ex vivo* porcine artery experiment [5]. Below, we report new findings in optimizing the magnetic properties of SPIO-RL platelets, which can be greatly enhanced by increasing SPIO uptake, leading to an improved MMOCT imaging contrast and threshold for detection.

Optical Coherence Tomography and Coherence Domain Optical Methods in Biomedicine XVI, edited by Joseph A. Izatt, James G. Fujimoto, Valery V. Tuchin, Proc. of SPIE Vol. 8213, 82131N

2. MATERIALS AND METHODS

2.1 Preparation of SPIO-RL platelets in clot-like aggregates

We prepared SPIO-RL platelet aggregates containing a greater loading of SPIOs, for comparison with dispersed SPIO-RL platelets in our previous study [5]. Here, dextran-coated SPIOs were prepared by a previous method [18] in citrated saline and 0.91 mg Fe/ml. The resulting dextran-coated SPIOs are expected to have core sizes of 10-20 nm, an outer diameter of 30-40 nm, and 50% Fe content by weight. As a comparison, in our previous study, Feridex I.V.® (Advanced Magnetics) is a dextran-coated SPIO with a core size of ~5 nm, ~60% Fe content by weight, and a hydrodynamic diameter of 36 nm.

In order to prepare the SPIO-RL platelets, they were incubated at an equal volume of prepared SPIOs with one-day old apheresis platelets, at a concentration of $1.1\times10^9/\text{cm}^3$. The SPIO platelet aggregates were subsequently separated from single platelets and free SPIO via differential sedimentation velocity and density gradient centrifugation, and then were subjected to aldehyde stabilization and lyophilization [6]. We examined them with light microscopy and found that SPIO-RL platelets were aggregates with a structure typical of primary hemostatic clots.

2.2 Magnetic properties measurements of SPIO-RL platelets

SQUID (superconducting quantum interference device) magnetometry was used to measure the magnetic properties of SPIOs and SPIO-RL platelet aggregates, and to compare them to freely dispersed SPIOs. We employed a 5T SQUID magnetometer (Quantum Design). SPIOs and SPIO-RL platelets were dispersed into 1% w/v agarose and sealed in a plastic capsule for analysis. Magnetization versus field $M(H)$ hysteresis loops were measured at 20°C, and subsequent calibration and subtraction of the diamagnetic contribution from the agarose and plastic capsule was computed as described previously [5]. The saturation magnetization, M_s, and an effective spin cluster magnetic moment, μ, were used as free-fitting parameters in the well-known Langevin function given by:

$$M(H) = M_s\left(\coth\left(\frac{\mu H}{k_B T}\right) - \frac{k_B T}{\mu H}\right), \tag{1}$$

where k_B is Boltzmann's constant, T is temperature, and the effective moment μ can be expressed in numbers of Bohr magnetons μ_B. Importantly, μ can be interpreted as the effective size of the superparamagnetic spin cluster, which determines the low-field magnetization and consequently the magnetically-induced force in MMOCT.

For further validation of the effective moment of SPIOs and SPIO-RL platelets, temperature-dependent field-cooled (FC) and zero-field-cooled (ZFC) magnetization was measured. The ZFC measurement was performed by first cooling to 5 K in nominal zero field (< 1 Oe), applying a 50 Oe field, and then measuring the DC magnetic response as the temperature was warmed to 320 K. In comparison, the FC scan was performed in 50 Oe as the temperature was cooled from 320 K back to 5 K. The blocking temperature was determined and the low-field magnetization was fit to the Curie law above the blocking temperature according to:

$$M(T) = \frac{\mu M_s}{3k_B T} H, \tag{2}$$

with μ as the only fitting parameter.

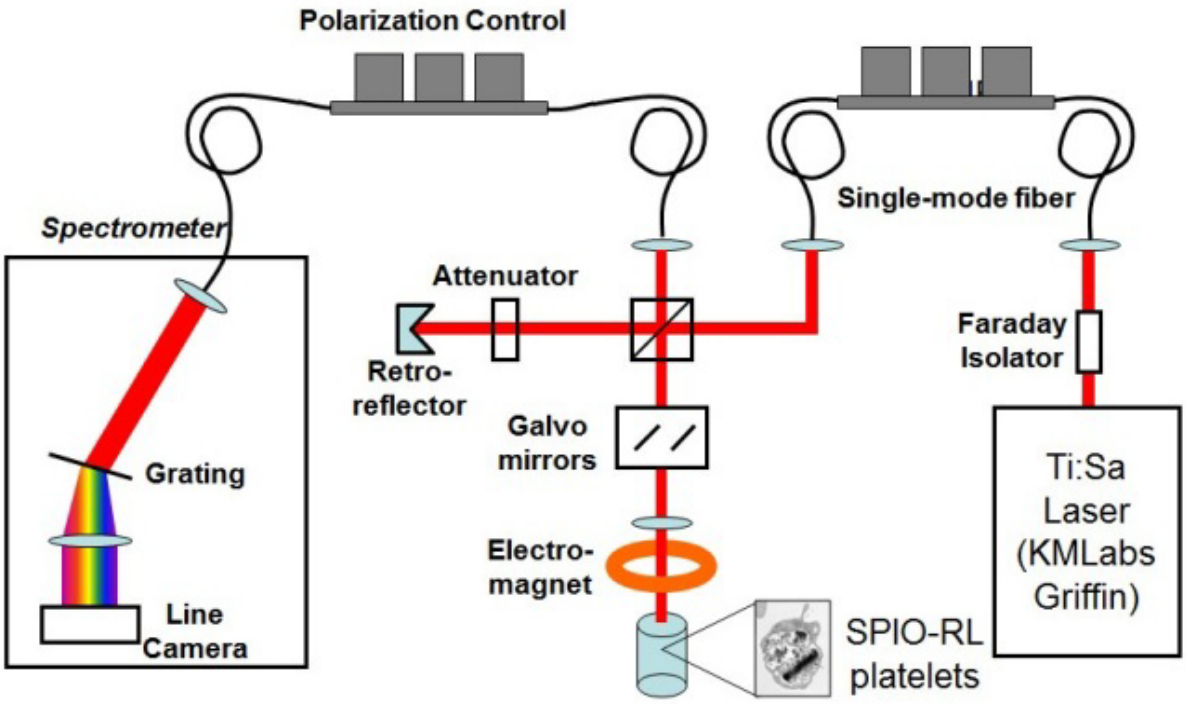

Figure 1. Figure captions are indented 5 spaces and justified. If you are familiar with Word styles, you can insert a field code called Seq figure which automatically numbers your figures.

2.3 Methods for MMOCT of SPIO-RL Platelets Phantoms

The methods used for magnetomotive OCT of SPIO-RL platelet aggregates are identical to those described previously [5]. To briefly summarize, a custom spectral-domain OCT system was constructed. This system is comprised of a Ti:Sapphire laser with a center wavelength of 810 nm and ~125 nm bandwidth (Griffin, Kapteyn-Murnane Labs). It also consists of a 30 mm focal length imaging lens which provided 3 × 12 μm (axial × transverse) imaging resolution. There was ~10 mW of optical power at the sample (Fig. 1). Images were collected into sequential B-mode frames over 2500 × 9 × 1024 pixels at an A-line rate of 1 kHz with the CCD camera (Dalsa Piranha 2). During acquisition, the magnetic field was modulated at 100 Hz. According to Hall probe measurements, the peak magnetic field and gradient were 0.15 T and 15 T/m, respectively. The OCT and MMOCT images were reconstructed using a phase-resolved method described previously. In this method, a bandpass filterer was used, and induced motions from the diamagnetic tissue background were removed by phase filtering [12].

3. RESULTS AND DISCUSSION

The new SPIO-RL platelet aggregates were found to contain >4× the amount of Fe per platelet, which was determined according to the saturation magnetization found with the SQUID magnetometry. As described above, the effective superparamagnetic spin cluster, μ, directly affects the susceptibility and thus the initial slope of the magnetization (in the M vs. H curve) at low field. Our findings were that the SPIO-RL platelets in this study displayed an effective spin cluster >3× larger than free SPIOs.

As a separate measurement of μ, temperature-dependent magnetization at low applied fields were obtained and fit to the Curie law in (2). Because these fields (50 Oe) are lower than those used in the field-dependent scans, the values are expected to be very close to the zero-field value of μ. Importantly, we found that μ from the temperature-dependent (low-field) scans are higher than that from the field-dependent (high-field) scans, but show the same enhancement for that of SPIO-RL platelets compared to that of the free SPIOs.

Importantly, the enhancement we observe in μ for the SPIO-RL platelet aggregates from free SPIOs was not observed for the SPIO-RL platelets in our previous study with Feridex I.V.®, where the values for μ are the same for both and only slightly larger than that of the prepared, free SPIOs in this study. Interestingly, this apparent increase in the effective magnetic cluster size for the SPIO-RL platelet aggregates is associated with a larger Fe loading, as well as an aggregated, clot-like nature. This suggests that magnetic interactions between SPIO particles are becoming significant.

In order to relate these magnetic property measurements to MMOCT contrast, MMOCT was performed of free SPIOs and SPIO-RL platelet aggregates dispersed in 1% agarose with 0.5–2mg/g TiO_2 micropowder as an optical scatterer. The measured magnetic properties of each sample were used to predict the induced magnetization at the peak modulation magnetic field of 0.15T used during MMOCT, while accounting for the negative magnetization from the diamagnetic background. In order to compare these samples with those measured previously, the Fe concentration was held constant at 67 µg/mL.

As expected, the predicted magnetization for each sample was strongly correlated with the resulting MMOCT contrast in tissue phantoms. Representative MMOCT images of free SPIOs and SPIO-RL platelet aggregates are displayed in Fig. 2. The highest contrast at 67 µg/mL was obtained for the SPIO-RL platelet aggregates, averaging 4.5±0.4 dB. Importantly, the platelet number density this corresponds to is only $0.31\times10^{9}/cm^{3}$, or over 4× less than the previous SPIO-RL platelets.

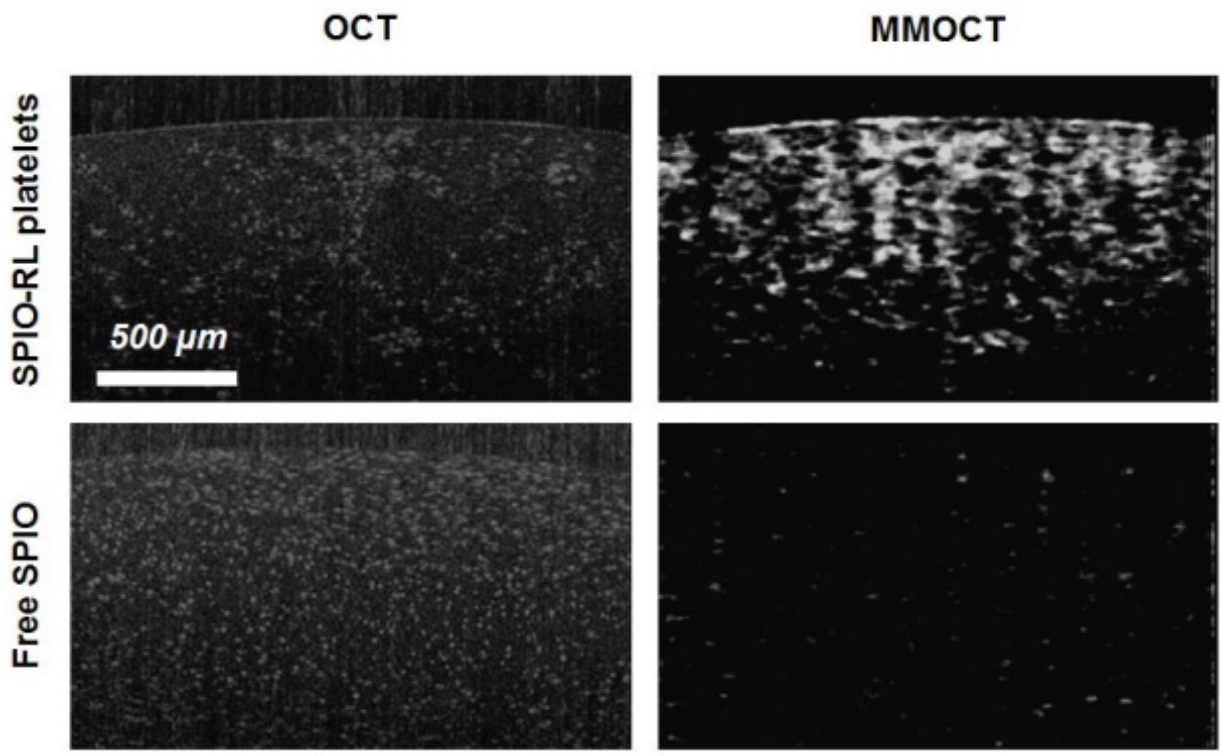

Figure 2. Example MMOCT images of SPIO-RL platelet aggregates compared to free SPIOs in agarose tissue phantoms.

4. CONCLUSION

These results suggest that the improved MMOCT contrast properties of SPIO-RL platelet aggregates are both a function of the improved Fe loading, and of particle-particle magnetic interactions, which improve their magnetic properties at the fields used in MMOCT imaging. Future study is needed to determine whether the aggregation of the platelets into a clot-like formation causes some of these improved properties, which may be a new mechanism of enhancing contrast *in vivo* that is activated when SPIO-RL platelets adhere to clots.

5. ACKNOWLEDGEMENTS

This work was supported in part by the U.S. Department of Defense under grant ONR N00014-10-1-0792 to ALO, the National Institutes of Health under grant R01HL094740 to ASW, NC TraCS UL1RR025747 with pilot Grants R61022 to ALO and R81034 to ASW, and startup funds at the University of North Carolina at Chapel Hill (ALO). The authors would like to thank R. K. Chhetri for his technical assistance with the construction and operation of the OCT system, and T. C. Nichols for providing porcine blood for magnetic analysis, both of whom are at the University of North Carolina at Chapel Hill.

REFERENCES

[1] I. K. Jang, B. E. Bouma, D. H. Kang *et al.*, "Visualization of coronary atherosclerotic plaques in patients using optical coherence tomography: comparison with intravascular ultrasound," Journal of the American College of Cardiology, 39(4), 604-9 (2002).

[2] G. J. Tearney, I. K. Jang, and B. E. Bouma, [Imaging coronary atherosclerosis and vulnerable plaques with optical coherence tomography] Springer, Berlin, 34 (2007).

[3] N. Burris, K. Schwartz, C. M. Tang *et al.*, "Catheter-based infrared light scanner as a tool to assess conduit quality in coronary artery bypass surgery," The Journal of thoracic and cardiovascular surgery, 133(2), 419-27 (2007).

[4] H. Azarnoush, S. Vergnole, R. Bourezak *et al.*, "Optical coherence tomography monitoring of angioplasty balloon inflation in a deployment tester," The Review of scientific instruments, 81(8), 083101 (2010).

[5] A. L. Oldenburg, C. M. Gallippi, F. Tsui *et al.*, "Magnetic and contrast properties of labeled platelets for magnetomotive optical coherence tomography," Biophysical journal, 99(7), 2374-83 (2010).

[6] M. S. Read, R. L. Reddick, A. P. Bode *et al.*, "Preservation of hemostatic and structural properties of rehydrated lyophilized platelets: potential for long-term storage of dried platelets for transfusion," Proceedings of the National Academy of Sciences of the United States of America, 92(2), 397-401 (1995).

[7] A. P. Bode, and M. S. Read, "Lyophilized platelets: continued development," Transfusion science, 22(1-2), 99-105 (2000).

[8] A. P. Bode, R. M. Lust, M. S. Read *et al.*, "Correction of the bleeding time with lyophilized platelet infusions in dogs on cardiopulmonary bypass," Clinical and applied thrombosis/hemostasis : official journal of the International Academy of Clinical and Applied Thrombosis/Hemostasis, 14(1), 38-54 (2008).

[9] H. Watarai, and M. Namba, "Capillary magnetophoresis of human blood cells and their magnetophoretic trapping in a flow system," Journal of chromatography. A, 961(1), 3-8 (2002).

[10] A. L. Oldenburg, J. R. Gunther, and S. A. Boppart, "Imaging magnetically labeled cells with magnetomotive optical coherence tomography," Optics letters, 30(7), 747-9 (2005).

[11] A. L. Oldenburg, S. A. Boppart, V. Crecea *et al.*, [Magnetomotive optical coherence tomography], U.S.(2010).

[12] A. L. Oldenburg, V. Crecea, S. A. Rinne *et al.*, "Phase-resolved magnetomotive OCT for imaging nanomolar concentrations of magnetic nanoparticles in tissues," Optics express, 16(15), 11525-39 (2008).

[13] J. Kim, J. Oh, T. E. Milner *et al.*, "Hemoglobin contrast in magnetomotive optical Doppler tomography," Opt. Lett., 31(6), 778-780 (2006).

[14] J. Oh, M. D. Feldman, J. Kim *et al.*, "Magneto-motive detection of tissue-based macrophages by differential phase optical coherence tomography," Lasers in surgery and medicine, 39(3), 266-272 (2007).

[15] J. Oh, M. D. Feldman, J. Kim *et al.*, "Detection of macrophages in atherosclerotic tissue using magnetic nanoparticles and differential phase optical coherence tomography," Journal of biomedical optics, 13(5), 054006 (2008).

[16] R. John, R. Rezaeipoor, S. G. Adie *et al.*, "In vivo magnetomotive optical molecular imaging using targeted magnetic nanoprobes," Proceedings of the National Academy of Sciences of the United States of America, 107(18), 8085-90 (2010).

[17] V. Crecea, A. L. Oldenburg, X. Liang *et al.*, "Magnetomotive nanoparticle transducers for optical rheology of viscoelastic materials," Optics express, 17(25), 23114-22 (2009).

[18] R. S. Molday, and D. MacKenzie, "Immunospecific ferromagnetic iron-dextran reagents for the labeling and magnetic separation of cells," Journal of immunological methods, 52(3), 353-67 (1982).